Helicopter vs. Volcanic Tremor: Characteristic Features of Seismic Harmonic Tremor on Volcanoes

Eva P. S. Eibl[1,2] (eva.eibl@ucdconnect.ie), Ivan Lokmer[1], Christopher J. Bean[2], Eggert Akerlie[3], Kristín S. Vogfjörd[4]
1: Seismology Laboratory, School of Geological Sciences, University College Dublin, Belfield, Dublin 4, Ireland
2: Geophysics Section, School of Cosmic Physics, Dublin Institute for Advanced Studies, 5 Merrion Square, Dublin 2, Ireland
3: Þyrluþjónustan ehf, Helo, Morkinni 3, 108 Reykjavík, Iceland
4: Icelandic Meteorological Office, Bústaðavegi 7 - 9, 108 Reykjavík, Iceland

1 Abstract

We recorded high-frequency (> 10 Hz) harmonic tremor with spectral gliding at Hekla volcano in Iceland. Particle motion plots indicated a shallow tremor source. We observed up to two overtones beneath our Nyquist frequency of 50 Hz and could resolve a source of closely spaced pulses of very short duration (0.03 - 0.1 s) on zoomed seismograms. Volcanic tremor with fundamental frequencies above 5 Hz, frequency gliding and/or repetitive sources similar to our observations were observed on different volcanoes around the world. However, this frequency content, duration and occurrence of volcano-related tremor was not observed in the last 35 years of seismic observations at Hekla. Detailed analysis reveals that this tremor was related to helicopters passing the volcano. This study relates the GPS track of a helicopter with seismic recordings of the helicopter at various distances. We show the effect the distance, number of rotor blades and velocity of the helicopter has on the observed up and down glidings at up to 40 km distance. We highlight similarities and differences between volcano-related and helicopter tremor in order to help avoid misinterpretations.

2 Introduction

When recording seismic tremor on volcanoes, it is crucial to distinguish between volcanic and other tremor sources. Possible sources not related to the volcano include but are not limited to ship propellers (Franek et al., 2014), animals such as whales (Pontoise and Hello, 2002), T waves (Talandier and Okal, 1996), icebergs (Müller et al., 2005; Talandier et al., 2002), subglacial water flows (Winberry et al., 2009; Röösli et al., 2014), lahars (Kumagai et al., 2009), ocean gravity waves and imperfectly designed recording units (Olofsson, 2010). Attempts to distinguish those sources focus on their fundamental frequency, strength and amount of overtones and the length and temporal changes of the tremor.
Harmonic volcanic tremor is usually observed between 1 and 9 Hz with a fundamental frequency around 1 Hz (McNutt, 1992; Soosalu et al., 2005; Gudmundsson et al., 1992) and integer harmonic overtones (Hotovec et al., 2013; Schlindwein et al., 1995; Hellweg, 2000). However, harmonic tremor with fundamental frequencies above 5 Hz was observed at Fogo (Heleno et al., 2006), a mud volcano in the SW Barents Sea (Franek et al., 2014) and a fundamental frequency of 10 Hz with 3 overtones was detected at a submarine

volcano in the Pacific (Dziak and Fox, 2002). Mt. Semeru volcano in Indonesia, Lascar volcano in Chile and Arenal volcano in Costa Rica are also exceptional due to overtones at more than 10 Hz (Schlindwein et al., 1995; Hellweg, 2000; Hagerty et al., 2000).

Strong up and/or down gliding was recorded at Arenal Volcano, Costa Rica (Benoit and McNutt, 1997; Hagerty et al., 2000; Almendros et al., 2012); Mt. Veniaminof, Alaska (De Angelis and McNutt, 2007); Monserrat, West Indies (Jousset et al., 2003); and Redoubt volcano, Alaska (Hotovec et al., 2013). Fundamental frequencies for these gliding events were between 1.9 and 3.4 Hz (Benoit and McNutt, 1997), between 1 and 3 Hz (Hagerty et al., 2000), between 1 and 2 Hz (Almendros et al., 2012), between 0.5 and 2 Hz (De Angelis and McNutt, 2007), and between 1 and 4 Hz (Jousset et al., 2003). Redoubt volcano is an exception as gliding frequencies spanning the range from less than 1 Hz to 30 Hz were observed. Up glidings typically started at a fundamental frequency of either 1 or 5 Hz (Hotovec et al., 2013).

Some source models explain volcanic tremor with and without frequency gliding with repeating pulses at uniformly increasing/decreasing or constant spacing (comb function), respectively (Schlindwein et al., 1995; Powell and Neuberg, 2003; Hotovec et al., 2013; Jousset et al., 2003). However, on volcanoes, the predominant models for tremor generation are related to sub-surface fluid motion in conduits (e.g., Chouet (1986), Jousset et al. (2003), Jellinek and Bercovici (2011), Julian et al. (1994), Rust et al. (2008)).

We demonstrate that some characteristics, in particular the repetitive source, fundamental frequencies and gliding lines of helicopter-generated tremor can be identical to those observed in volcanic tremor. In such cases, one could misinterpret the helicopter-generated tremor as volcanic tremor if special care is not taken. In the following, we provide a detailed analysis of helicopter-generated tremor and give guidelines for preventing misinterpretations.

3 Tremor Observations at Hekla Volcano

Hekla volcano lies at the connection between the South Iceland Seismic Zone and the Eastern Volcanic Zone (e.g., Einarsson (1991)). Volcanic tremor accompanied all recent eruptions in 1980/81, 1991 and 2000, commencing and ending sharply with the eruption (Grönvold et al., 1983; Gudmundsson et al., 1992; Soosalu et al., 2005). In 1980/81 the harmonic tremor correlated well with the tephra production rate (Grönvold et al., 1983). In 1991, a tremor band from 1 to 3 Hz (maximum around 2.5 Hz), propagating as Rayleigh and Love waves at a speed of 500-1000 m/s, correlated with the force of the eruption (Gudmundsson et al., 1992). The volcanic tremor during the eruption in 2000 was similar to the 1991 tremor with one to three major peaks between 0.7 and 0.9 Hz. Subdominant peaks were detected between 0.5 and 1.5 Hz from time to time. In comparison to detected earthquakes, tremor was attenuated faster and could hardly be detected at stations at more than 65 km distance. This was attributed to a shallower source. This was also supported by particle motion studies which identified Rayleigh waves. The tremor amplitude was strongest at the beginning of the eruption and roughly correlated with plume height (Höskuldsson et al., 2007). At later stages, the tremor decreased as the explosive activity decreased. Importantly there are no reports of tremor outside periods of eruptive activity at Hekla.

We were interested in the background seismicity on Hekla volcano and installed five temporary Güralp 6TD seismometers, operational between August 9 and October 10, 2012 (figure 1).

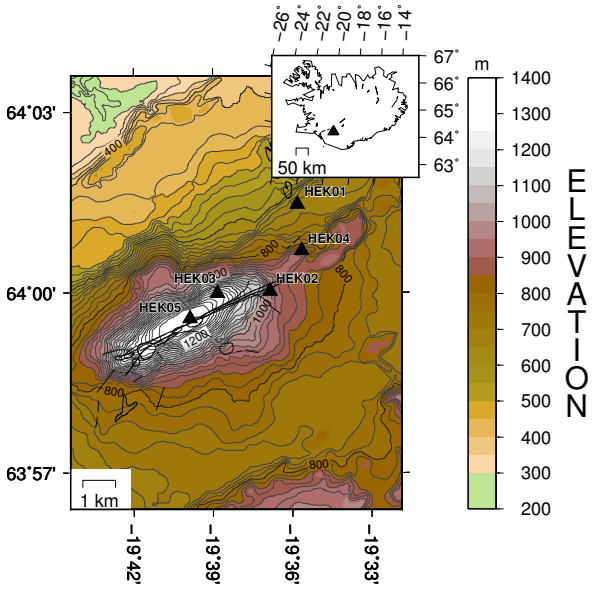

Figure 1: Location of temporary deployed seismometers on Hekla volcano. Elevation is a.s.l.

Apart from recently detected microseismicity (Eibl et al., 2014), it is usually described as aseismic in periods of quiescence (Soosalu and Einarsson, 2002; Soosalu et al., 2005; Grönvold et al., 1983).

Nevertheless, we observed 42 seismic tremors on all five stations which are pulsating and have emergent onsets in the time domain (see figure 2c). The envelopes of the tremor are quite different from station to station, although within a 2 s long window, we can resolve repeating pulses on all stations.

In the frequency domain, down gliding is observed with an inflection point and equally

spaced overtones up to the Nyquist frequency of 50 Hz. Depending on the fundamental frequency, 0-2 overtones are visible below the Nyquist frequency at integer multiples of the fundamental frequency. We observed three groups of glidings around three different fundamental frequencies. The most common gliding starts at 22-25 Hz and falls to 14-18 Hz (figure 2a, overtone not shown). Another common gliding starts at 30-34 Hz and falls to 21-25 Hz (figure 2b), and a third group starts at 15-17 Hz falls to 11-14 Hz (figure 2c). No difference in the amplitudes between the fundamental frequency and higher harmonics was observed.

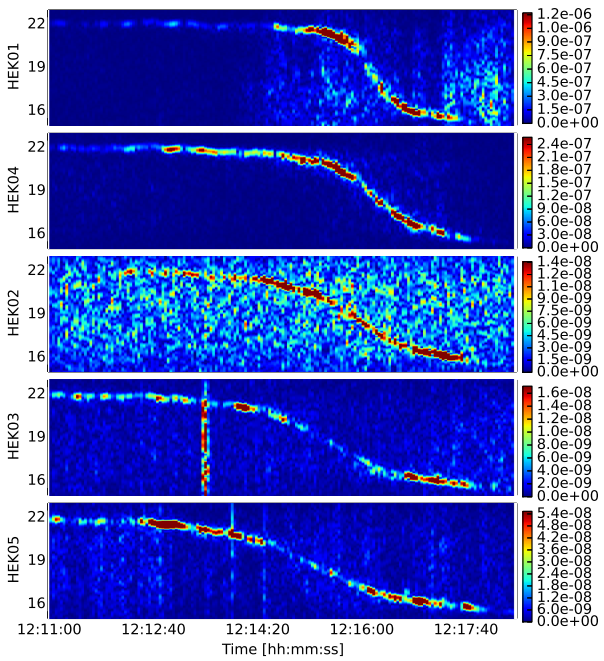

(a) August 25^{th}, 2012 12:11:00 - 12:18:00

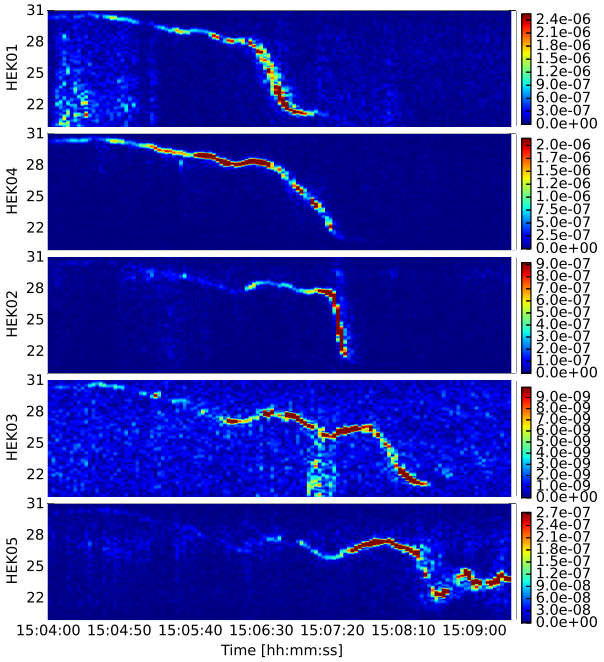

(b) August 13^{th}, 2012 15:04:00 - 15:09:30

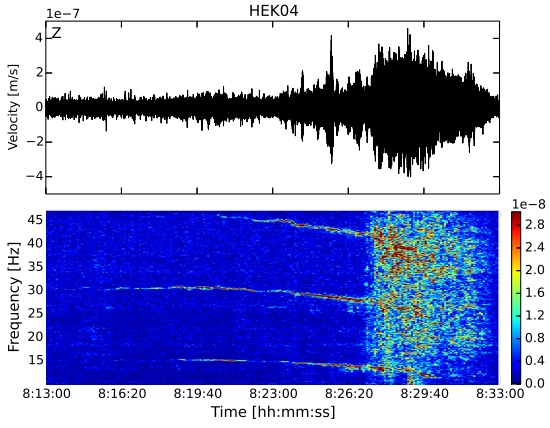

(c) September 19^{th}, 2012 8:13:00 - 8:33:00

Figure 2: Spectrogram of the vertical components of all five Hekla stations on (a) August 25, 2012, at 12:11:00-12:18:00 filtered 15-23 Hz and (b) August 13, 2012, at 15:04:00-15:09:30 filtered 21-31 Hz. Colors indicate the Power Spectral Density of the signal. (a) Strong change in slope, (b) Clear propagation in time, (c) Seismogram and spectrogram of the vertical component on September 19, 2012, filtered 11-47 Hz showing slow gliding with a fundamental frequency around 13 Hz and 2 overtones.

At neighboring stations, gliding patterns are similar but slopes are different. We mostly observed the fastest gliding at the station with the strongest signal. The seismic signal was usually lost shortly before and after the gliding. Some glidings, however, were preceded or followed by up to 15 min by a persistent non-gliding spectral pattern. Moreover, two tails could be observed in rare cases.

4 Data Analysis

4.1 Initial Tremor Analysis at Hekla

Initially, we analysed the tremor assuming a volcanic source. Zooming in reveals a source consisting of short duration, repeating pulses (figure 3).

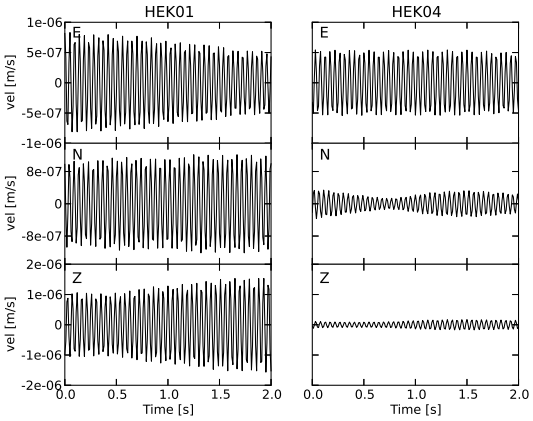

Figure 3: Seismogram of the tremor at (left) HEK01 and (right) HEK04 on August 25, 2012, from 12:15:08 to 12:15:10 filtered from 20 to 23 Hz.

In figure 2, we show 3 different signals, with fundamental frequencies around 13, 20 and 26 Hz, respectively. Figure 3 shows the corresponding signals in the time domain for a part of figure 2a. By comparing the two figures, it can be seen that the fundamental frequency (as well as the separation between the fundamental frequency and higher harmonics) is equal to the reciprocal value of the time interval between successive pulses. Since the repeating period of individual pulses is longer than $1/f_{Nyquist}$ and individual pulses are shorter than $1/f_{Nyquist}$, the higher harmonics are present all the way up to the Nyquist frequency, as in the case of the delta comb function.
Particle motion plots indicate the retrograde elliptical motion of Rayleigh waves as further discussed in section 4.4. This suggested a likely shallow source which is consistent with tremor observations during eruptions at Hekla. However, previous tremor was always strongly linked to explosive activity during an eruption. We expect a shallow tremor source to be coincident with changes in deformation data, strain measurements or possibly gas measurements. A lack of correlation of our tremor observations with these observables made us suspicious of a volcanic origin. This tremor was also at higher frequency, observed only between 8:24 am and 11:22 pm and during a period of volcano quiescence. However, tremor has not been observed during a period of volcano quiescence in the previous 35 years of instrumental recordings at Hekla. Comparing the time of the inflection points at all stations, it sometimes seemed that the source moved in time (see figure 2b), whereas in others, it did not (see figure 2a). Thus, we searched for recordings of this signal

at a permanent station from the Icelandic Meteorological Office network in Haukadalur (63.9685 N, 19.9647 W) 15 km west of Hekla. Surprisingly - still assuming a volcanic tremor source - this high-frequency tremor could be observed, but it was usually about 4 min earlier than at the stations on Hekla. It transpired that the sources were helicopters in the vicinity of Hekla volcano.
Our concern is that these signals could readily have been interpreted as exotic, volcano-related signals. Although experienced observatory staff would likely identify the signals as cultural noise, this is not necessarily the case for intrepreters in general. This might be especially true at volcanoes that are poorly monitored (in a seismo-acoustic sense). With a single station (or several stations in a unfavorable position with respect to the source of tremor), it may be difficult to distinguish the Doppler effect from temporal variations of a volcanic source. In section 4.3, we link the different features visible in the spectrograms to the GPS track of a helicopter that we acquired in December 2014. This experiment was carried out with permanent stations at a different location. The helicopter performed a flyby in the vicinity of two seismic arrays, deployed west of Vatnajökull glacier. We also compared the characteristics of these signals to those of volcanic tremor.

4.2 Station Network and the Helicopter GPS Track

A comparison of the seismic data and the GPS track of the helicopter was undertaken with two seven-station broadband arrays with an aperture of 1.6 km in Jökulheimar and Innri Eyrar, near Laki west of Vatnajökull glacier (figure 4b). The arrays include six Güralp 6TD sensors and one Güralp 3ESPDC at the array center (JOK and IEY in figure 4b).
We have the GPS track (figure 4a) of a four-bladed helicopter on December 19, 2014. The instrument is a Garmin 795 with an accuracy of at least 10 m and a sampling rate of 5 Hz. In the 'smart sampling', mode points were saved every 1-18 s in order to both save memory and record changes in the heading. The helicopter was less than 50 km away from Jökulheimar between approximately 11:00 and 12:15 UTC. The helicopter crossed the array in Jökulheimar at 11:53:30 flying westwards from Þórðarhyrna. According to the manufacturer, the rotor revolutions per minute (RPM) is fixed at 413 (6.883 Hz) for this helicopter model. The wind speed was 5 m/s from the north. From the GPS track, we calculated a speed of 210 km/h and a flight direction of 253.55° from north directly above the array. The helicopter crossed the array north of JOG and south of all the others closest to stations JOA, JOK and JOD at 960 m height a.s.l. (figure 4b), which corresponds to 220 to 280 m above the array.

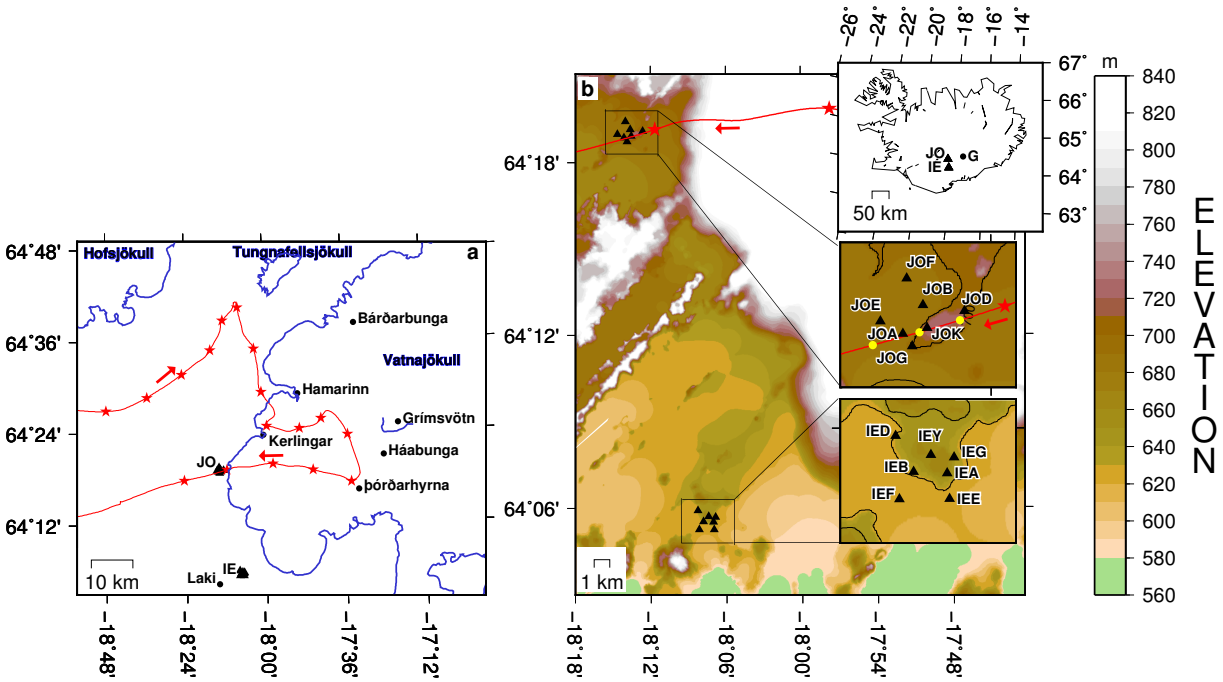

Figure 4: (a) The GPS track of the helicopter is shown in red, where red stars are 3 min apart and mark the helicopter location at the time ticks in figure 5. The flight direction is indicated with red arrows. Volcanoes, glaciers and the arrays JO and IE are marked for orientation. (b) Location of seismometers arranged as 7-element arrays in Jökulheimar and Innri Eyrar near Laki. Red track as in a. The insets show (top) the arrays JO and IE with respect to the whole island and Grimsvötn marked with G, (middle) the geometry of JO. Yellow dots mark the helicopter position at 11:53:14, 11:53:28 and 11:53:44 for reference to the particle motion plots shown in figure 8 and (bottom) the geometry of IE. Elevation is a.s.l.

4.3 Spectral Gliding

4.3.1 Linking Seismic Observations and Helicopter Position

Figure 5 shows the seismic recording at JOA while the helicopter followed the track in figure 4a where the stars indicate the times labeled in figure 5. Together with the seismogram and spectrogram, we show the helicopters distance to station JOA, as well as its speed and azimuth. When calculating the distance, we included horizontal distance as well as the height difference. We detected the helicopter three times during this period, including 11:09:00 to 11:16:00, 11:24:30 to 11:33:30 and 11:46:00 to 11:54:00. First as a slow down gliding, second as a combination of up and down glidings that end in a steep down gliding and third as a very strong, steep down gliding which is preceded by a slow up gliding. Up and down glidings are a consequence of the distance between helicopter and seismometer, the velocity and azimuth as we will describe below.

The seismometers in Jökulheimar record the helicopter for the first time at 29 km distance while it flew northeastwards towards Tungnafellsjökull (see figure 4a). In the following 7 min, the distance between the helicopter and the seismometer first decreases to a minimum of 25 km and then increases to 30 km. While the helicopter continued towards Tungnafellsjökull, we lost its seismic signal.

The second recording starts after the helicopter changed direction close to Tungnafellsjökull from northeast to south-southeast and approaches the seismometers again. The signal is detected when the helicopter is still 36 km away. The following 9 min are characterized by speeds between 210 and 233 km/h, azimuths between 140 and 180° and a distance decreasing from 36 to 16 km. Changes in these three parameters create a seismic

signal of multiple up and down glidings that span less than 5 Hz. When the helicopter changes direction from SSE to E close to Kerlingar (see figure 4a), the distance increases again and the signal is lost at 20 km distance.
The third recording starts 2 min after the helicopter turned around near Þórðarhyrna at a distance of 29 km. From there, the speed and azimuth are about constant and the helicopter flies westwards crossing the array around 11:53:30. Fluctuations in speed and azimuth and a slow increase in speed show up as small fluctuations in the frequency before the final strong Doppler glide, when the helicopter flies directly over the array.

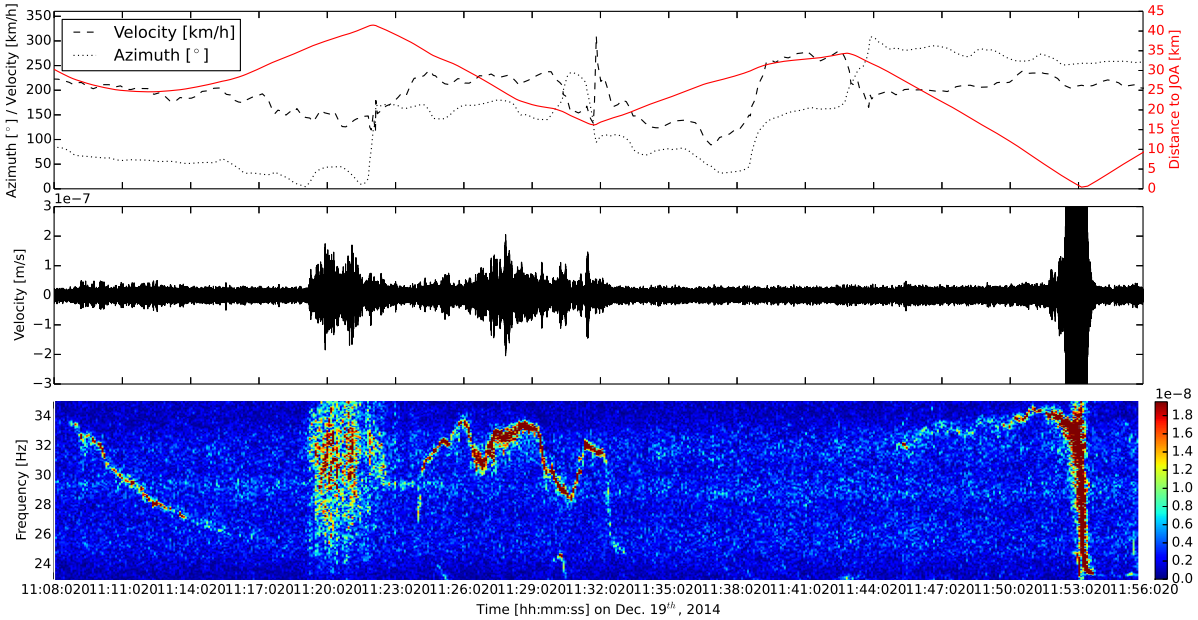

Figure 5: (top) Flight direction of the helicopter as azimuth measured clockwise from north (dotted line), velocity of the helicopter (dashed line) and distance between the helicopter and station JOA (red solid line). (middle) Instrument corrected and 23-35 Hz filtered seismogram of the vertical component at JOA in Jökulheimar clipped at $3{\cdot}10^{-7}$ m/s. (bottom) Spectrogram of the displayed seismogram showing the gliding of the fundamental frequency.

4.3.2 Analysis of Doppler Gliding: Methodology

It is possible to describe the frequency and velocity of a moving acoustic source relative to a fixed receiver using the following equations if the source is approaching the receiver directly (Feynman et al., 1963):

$$f_{bh} = \frac{f_s}{(1 - \frac{v_{sr}}{c})} \tag{4.1}$$

for the approach and

$$f_{bl} = \frac{f_s}{(1 + \frac{v_{sr}}{c})} \tag{4.2}$$

for the departure, where f_s and v_{sr} are the acoustic source frequency and radial velocity of the helicopter, respectively, c is the sound speed of 340 m/s and f_{bl} and f_{bh} are the lower and upper frequency observed. For an arbitrary flight direction, we can replace v_{sr} with $v_s \cdot cos\Phi$, where v_s is the velocity of the source and Φ is the angle between the receiver-source direction and the flight direction. Considering geometrical relationships between the receiver position and the helicopter's trajectory, $cos\Phi$ can be further replaced

with $\frac{v_s \cdot t_n}{\sqrt{(v_s \cdot t_n)^2+h^2}}$, where h is the closest distance between source and receiver and t_n is the time which is 0 at closest approach. The general representation of the curve is

$$f(t) = \frac{c \cdot f_s}{c + \frac{v_s^2 \cdot (t-t_0)}{\sqrt{v_s^2 \cdot (t-t_0)^2+h^2}}} \tag{4.3}$$

where f(t) is the observed frequency with respect to UTC time t, and t_0 is the time at which the helicopter is closest to the stations (at distance h).
Analysis of typical Doppler gliding in the spectral domain allows us to deduce the helicopter speed, blade rotation frequency and number of blades using equation 4.3. Processing steps include the removal of the seismic instrument response and band-pass filtering the signal to the frequency band of interest (e.g., 22-36 Hz). We then calculate spectra over 2.4 s long time windows with 98% overlap. We chose this time window as it resulted in a smooth curve and a good frequency resolution suitable for curve fitting. We pick the lowest (fundamental) peak in the amplitude spectrum and use the resulting time series for all 7 stations as basis for the following analysis.
Fitting the curves with equation 4.3 gives us an estimate of t_0, f_s, v_s and h. We can compare v_s directly with the helicopter properties and convert f_s to RPM. The resulting RPM will be the product of the RPM of the helicopter multiplied by the number of blades. As a standard RPM is in the range 385-415 RPM (6.417-6.917 Hz), it is therefore possible to deduce the number of blades from the RPM we calculate. The other properties can be used to locate the helicopter and determine its flight direction as shown in Lo and Ferguson (2000). This is beyond the scope of this study.
Additional information can be gained from the shape and length of the source pulses when analyzing the overtones of the signal. The spacing of the overtones corresponds to the time interval between repeating sources (Båth, 1974). The attenuation of overtones contains information about the shape of the amplitude spectrum of a single source pulse. Effectively, the recorded signal is the convolution of the source pulse (a pressure pulse produced by a single blade) with an infinite comb function (repetitive action generated by the rotation of the blades). For overtones to be visible, their frequency must overlap with the spectrum of the single pulse.

4.3.3 Slope of the Doppler Gliding with Respect to Distance

From 11:52:20-11:54:10, we recorded the helicopter on all seven stations in Jökulheimar and three out of five stations in Innri Eyrar (two stations were in acoustic shadow). The gliding slopes are steeper for stations closer to the helicopter flight path. In figure 6 the slopes range between -0.72 Hz/s (JOA) and -0.24 Hz/s (JOF). Figure 6 shows the frequency that contains the highest power in the spectrum of a 2.4 s long time window that overlaps 98% with the next one and the root mean square (RMS) of the amplitude in the same time windows. Note that the time of closest approach is not the time of the highest amplitude (figure 6) and that amplitude distribution is not smooth. In fact JOK and JOD - the stations directly below the helicopter - have unusually low amplitudes (see figure 4b for the GPS track and figure 6 for the amplitudes). Using equation 4.3, we calculate a RPM of 418.8 ± 24.4 for a four-bladed helicopter that flew at 222 ± 9 km/h. The estimated error is based on the frequency resolution visible in figure 6 and converted to RPM and velocity. The results are consistent with a known RPM of 413 according to the manufacturers and a known speed of 209.66 km/s derived from the GPS track.

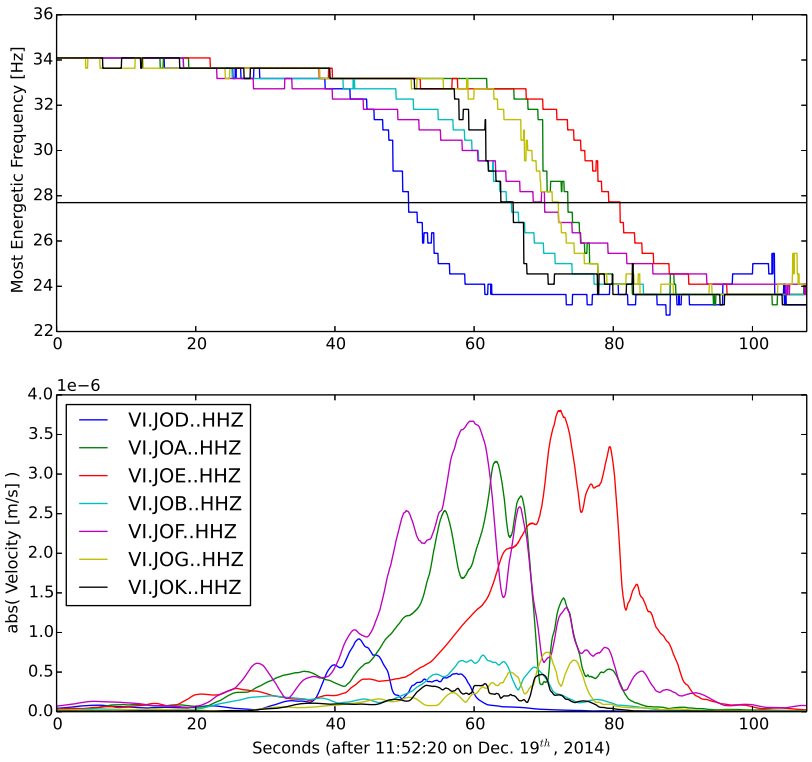

Figure 6: Spectral analysis of the vertical component of the stations in Jökulheimar. Spectra and RMS were calculated in 2.4 s long time windows overlapping by 98%. (top) Most energetic frequency of the spectrum of each 2.4 s long time window at all station of the JO array. (bottom) RMS of the 2.4 s long time windows at all stations in the JO array.

For the stations at greater distances, we expect slow or no visible gliding as in figure 2c. This is due to very small changes in the relative source-receiver distance. In Innri Eyrar (figure 7), we observed in fact a weak signal that glided slowly downwards between 11:41:00 and 11:56:00. However, the general frequency gliding was overlain by frequency fluctuation of up to $\pm$ 1 Hz.

We note that the array in Innri Eyrar recorded the helicopter at 40 km distance at 11:41:00, whereas the array at Jökulheimar at less than 35 km distance did not. In Jökulheimar, it was recorded 5 min later at only 29 km distance. This might be due to the wind direction from the north (5 m/s). However, only the stations in Innri Eyrar on the northwestern side of the hill recorded it (except for IED, where the noise level was too high). The stations a few hundred meters further southeast were sheltered from the pressure wave by the hill or a cliff (see figure 4).

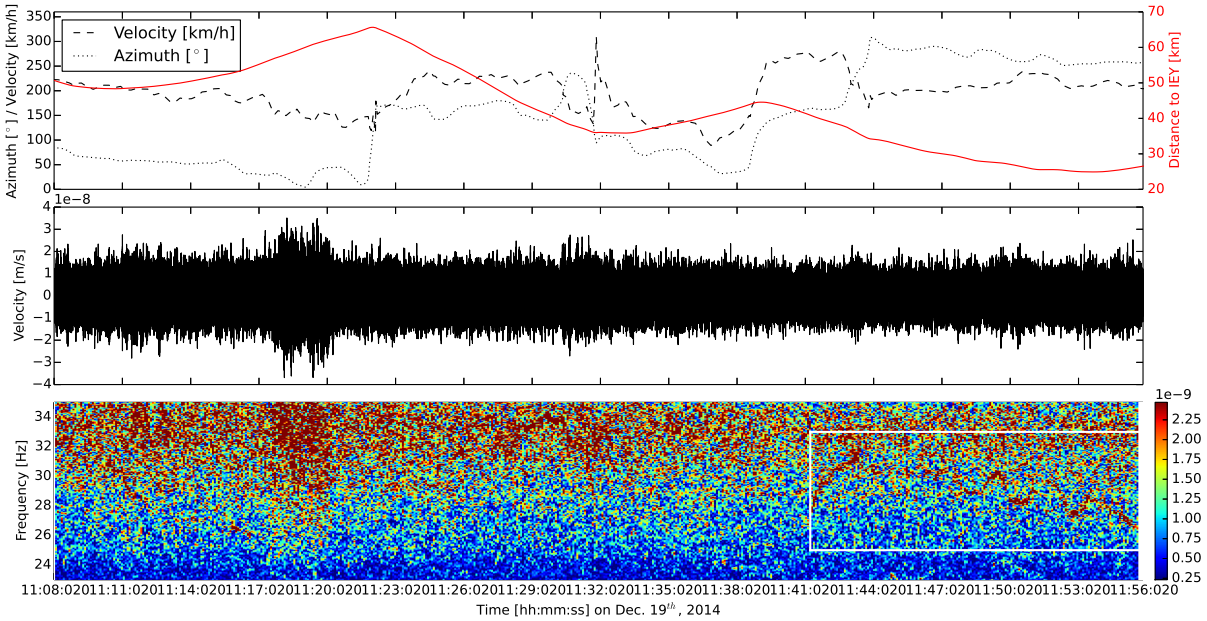

Figure 7: Same as figure 5 but for station IEY in Innri Eyrar. The white box mark the helicopter signal.

4.4 Particle Motion Analysis

The main rotor's blades create an acoustic signal. These repeating pressure pulses travel through the air and decay in amplitude. Due to a strong attenuation of high frequencies in the ground, we conclude that the recorded waves are excited close to the seismometer. The average noise level (RMS) on the analyzed day in the shown frequency band was $3.6{\cdot}10^{-9}$ m/s at IE and $5.9{\cdot}10^{-9}$ m/s at JO. Although in the spectrograms we were able to visually identify signals with a signal-to-noise ratio down to 1.05 (see figure 7), quantitative analysis of the signal undertaken, e.g., in figure 6, was carried out with a signal-to-noise ratio of 13.8. This sensitivity is high due to a low noise level on that day, e.g., due to low wind speeds.

When zooming into the seismogram, we can resolve the pulses created by the rotor blades. We show four 1 s or 0.5 s long particle motion plots from JOB (figure 8a-d) in the time window 11:53:13 to 11:53:32.5. We observe a longer and a shorter period oscillation. At all stations, the longer period oscillation is an elliptical-retrograde wave, propagating in the vertical plane (N-Z and E-Z subplots in figure 8). This plane is oriented NW-SE when the helicopter approaches the stations from the east (N-E subplot in figure 8a and b). It changes to N-S at the time of closest approach (figure 8c) when the helicopter is south of JOB and changes to NE-SW when it departs towards the west (figure 8d). This implies that the helicopter creates Rayleigh waves through atmospheric coupling to the ground (Bass et al., 1980). The shorter period oscillation has a period of 0.04 s in this time window and correspond to the individual pulses from the rotor blades.

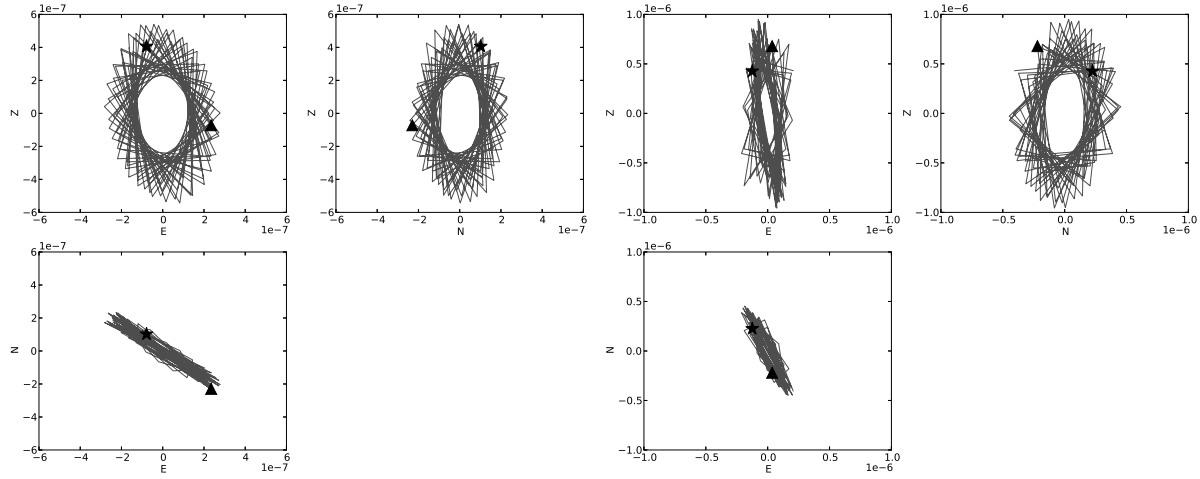

(a) 11:53:13-11:53:14 (b) 11:53:20-11:53:21

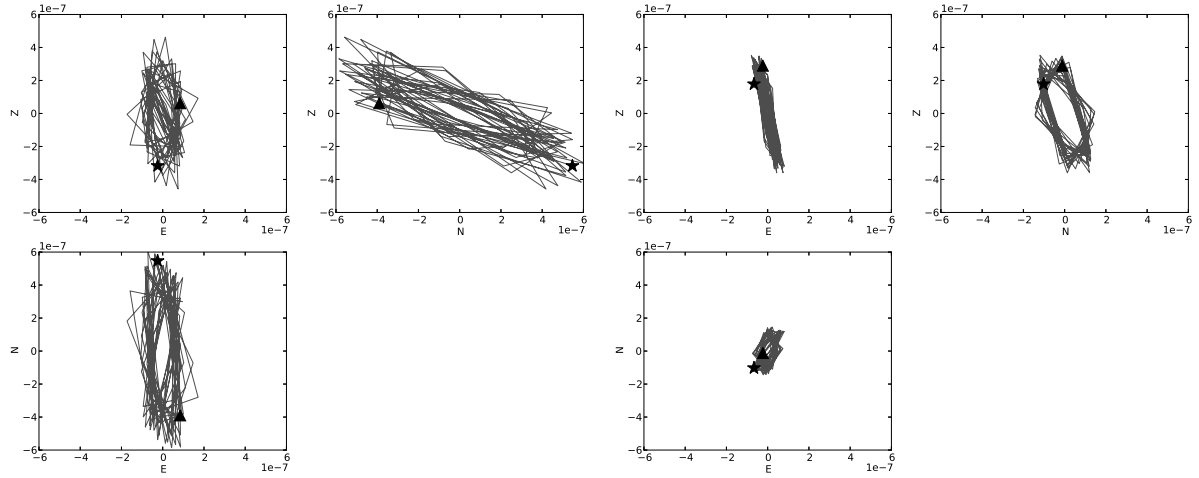

(c) 11:53:27-11:53:28 (d) 11:53:32-11:53:32.5

Figure 8: (a-d) Particle motion plots (velocity in m/s, filtered 22-36 Hz) for station JOB at (a) 11:53:13-11:53:14, (b) 11:53:20-11:53:21, (c) 11:53:27-11:53:28 and (d) 11:53:32-11:53:32.5. The corresponding position of the helicopter at panels a and c is marked with a yellow dot in figure 4b. The black star and triangle mark the first and second time sample, respectively. Note the different scale in panel b.

5 Summary of Results and Discussion

In general, helicopters in Iceland have a main rotor with two, three or four blades. These blades turn at a rate of 385 to 415 RPM (6.417-6.917 Hz) and create repeating pressure pulses. These pulses are created when a blade passes through a tip vortex shed by a previous blade, as further discussed in, e.g., Malovrh and Gandhi (2005) and Hardin and Lamkin (1987). The tail rotors often turn at 2100-2500 RPMs (35-41.7 Hz) with two blades usually not creating much noise on cruise flights as they do not create much lift at that stage. At maximum speed of 200-300 km/h the rotor RPM does not vary by more than 1-2%. The frequency at which pressure pulses emanate from the helicopter is the RPM times the number of blades. It equates to 12.8-13.8, 19.25-20.75 and 25.6-27.7 Hz for a two, three or four-bladed helicopter, respectively (recordings were published in Damarla and Ufford (2008); Damarla (2010)).

We recorded the regularly repeating pressure pulses generated by helicopter rotor blades with seismometers. As the source moved and passed our stationary recorder, we observed Doppler gliding in the frequency domain with inflection points around the above mentioned frequencies. All harmonics are visible at the same amplitude, e.g., figure 2c, which led us to the conclusion that the frequency content of the single pulse is approximately flat between the fundamental and Nyquist frequencies. For the four-bladed helicopter observed in this work, the spacing between those pulses was between 0.029 s and 0.042 s. A seismic recording of a helicopter with a spacing of about 0.08 s can be seen in Damarla and Ufford (2008). Particle motion plots indicate that the long period ground oscillation is a retrograde Rayleigh wave.

We observed that a seismometer a few hundred meters away recorded a higher amplitude than a seismometer directly below the helicopter. We have access to another flyover where the helicopter was a few hundred meters south of all stations in Jökulheimar and where we observed the amplitude decaying with increasing distance to the source as expected. Interestingly, we also observed that the amplitude of the signal was not strongest when the helicopter was closest to the seismometer (compare times of inflection points and maximum amplitudes in figure 6). Radiated pressure waves from the helicopter are shadowed immediately below the aircraft. A contributing factor to this effect is the acoustic-to-seismic coupling itself. At a certain angle, Rayleigh waves may be created more efficiently, especially if the angle allows for constructive interference of surface waves (Bass et al., 1980). HOwever, interference can also occur if the signal is reflected from a topographic feature. This has to be kept in mind for amplitude and phase/ travel time studies and might change or destroy gliding patterns.

In general, we observed that the distance alone is not the only factor that influences whether the signal is recorded. We often found or lost track of the helicopter at approximately 29 km distance for recordings in Jökulheimar. However, when coming from the north - which was the wind direction on that day - we recorded it even when 35 km away. In contrast we lost the signal at 19 km distance when the helicopter flew eastwards, north of the Kerlingar mountains. This is supported by recordings of the helicopter at 40 km distance at the Innri Eyrar array, which was located downwind on that day. This suggests that both wind direction and topography play an important role. This would also explain, why we observed tails prior to the gliding or following the gliding but only in rare cases both prior to and following the gliding.

We also want to note that up- or down drafts on windward or leeward slopes might affect the observed frequencies. They can lead to sudden height changes but also to an increase/ decrease in power to compensate for the draft. As the topography in our example is rather

smooth and the wind was weak, up- and downdrafts played a minor role in creating the observed frequency changes. This is confirmed by the observation that there is no correlation between height changes and frequency glidings.

We observed ground velocities on the order of 3.6 nm/s at 40 km distance (see figure 7) on a day with a low noise level and low wind speed. We inspected all our recordings in 2014 and found a maximum duration of 40 min for a helicopter-generated signal. Assuming a passing helicopter at a speed of 180-240 km/h, it would travel 120-160 km during that time. This implies that the pressure wave created by the helicopter blades is large enough to be recorded by seismometers at least 60 km downwind, assuming that it was closest to the stations after 20 min and travelling in a straight line.

In cases where the helicopter did not fly directly above the seismometer we observed slow Doppler glides, spectral lines at the frequency of the source, up glidings or a random combination of up and down glidings. Up glidings can be the consequence of a helicopter that is first flying away from the seismometer but then turning and flying towards it. This was shown in Damarla (2010), where a helicopter followed a track approaching and departing a sensor multiple times. A pattern of complex up and down glidings is probably the consequence of a combination of distance, altitude, velocity, azimuth and RPM of the helicopter. Slight variations in those parameters are normal but might be larger if the helicopter is on a sight-seeing tour or rescue mission.

Spectral analysis of a standard Doppler glide enabled us to deduce the speed, the number of rotor blades and RPM of the helicopter. We estimated a RPM of 418.8 $\pm$ 24.4 for a four-bladed helicopter that flew at 222 $\pm$ 9 km/h. This is in good agreement with a RPM fixed at 413 according to the manufacturer and a speed of 209.66 km/s, which we calculated from the GPS track. In the GPS track, we determined three occasions where the distance between the stations and the helicopter first decreased and then increased. During all those times we recorded Doppler glides at different speeds, amplitudes and start and end frequencies. The amplitudes are higher and gliding occurs faster if the helicopter is closer, which is in agreement with our expectations. The upper and lower frequency will be influenced by the velocity but if the source is too far away the signal will be too weak which makes it difficult to determine the exact higher and lower frequency of the gliding. An additional difficulty when determining the upper and lower frequency are rapid speed changes of the helicopter, visible, e.g., during the second gliding.

We can conclude that the shapes of helicopter tremors depend significantly on the distance and uniformity of velocity, flight direction and RPM of the source. Fundamental frequencies tend to be around 13, 20 and 28 Hz but can reach as low as 10 Hz.

Redoubt volcano is the perfect example for very similar volcano-related, harmonic tremor. Frequency up gliding was observed from less than 1 up to 30 Hz or 5 to 30 Hz prior to explosions, down gliding interrupted by small up glidings had fundamental frequencies above 5 Hz (Hotovec et al., 2013). Other strong up and down glidings (Benoit and McNutt, 1997; Hagerty et al., 2000; Almendros et al., 2012; De Angelis and McNutt, 2007; Jousset et al., 2003) and fundamental frequencies of more than 5 Hz were observed on various volcanoes (Heleno et al., 2006; Franek et al., 2014; Dziak and Fox, 2002). The latter can be similar to a helicopter passing a seismometer at a greater distance where no gliding but only the frequency of the rotor blades is observed.

Suggested models for volcanic tremor are repeating equally spaced pulses (Schlindwein et al., 1995; Powell and Neuberg, 2003; Hotovec et al., 2013; Jousset et al., 2003) and resonances of various sources (Franek et al., 2014; Dziak and Fox, 2002; Benoit and McNutt, 1997; De Angelis and McNutt, 2007; Schlindwein et al., 1995; Hellweg, 2000). If frequency gliding is observed, then it is attributed to a change in the source geometry in

the case of a resonating source, or a change in the spacing between pulses of a repeating source. This is in contrast to helicopter tremor where the observed change in frequency is merely an effect caused by the movement of the source relative to the receiver, not a change in the frequency of the source.

In order to distinguish helicopter tremor from a volcanic source, we suggest that a variety of observables be compared. The fundamental frequency of harmonic tremor would be around 13 Hz for a two-bladed helicopter and higher for helicopters with more blades or a RPM above 400. These frequencies are higher than observed at most volcanoes. Another characteristic is the duration of the signal. The longest helicopter signal we observed was 40 min long. Continuous volcanic tremor can persist on the order of hours to days. Particle motion plots that indicate Rayleigh waves whose orientation changes in time are typical for a helicopter but are rather unlikely for a volcanic source. Seismic amplitudes can reveal helicopter tremor as well. A first increasing, then decreasing seismic amplitude that is strongest near the inflection point of a down gliding will indicate a helicopter as source. Furthermore, we observed a strong link between the slope of the down gliding and the recorded signal amplitude for helicopters.

It is advisable to check the historical behaviour of a volcano and other observations, e.g., visual recordings of a volcano, its degassing behaviour or deformation measurements including GPS or satellites in order to check for correlations that support a volcanic source. In the case of Hekla volcano, the observed tremor signals in this study show no causal relationship with volcanic activity. We conclude that by analyzing the physical properties of the tremor in the time as well as the spectral domain and by comparing recordings from different disciplines or even microphone recordings it is possible to distinguish volcanic and helicopter tremor.

6 Acknowledgements

The data were collected and analyzed within the framework of FutureVolc, which has received funding from the European Union's Seventh Programme for research, technological development and demonstration under grant agreement No. 308377. We thank Martin Möllhoff for fruitful discussions. We also want to thank David Green and an anonymous reviewer for their critical comments that helped to improve the manuscript.

7 References

Javier Almendros, Rafael Abella, Mauricio Mora, and Philippe Lesage. Time-Dependent Spatial Amplitude Patterns of Harmonic Tremor at Arenal Volcano, Costa Rica: Seismic-Wave Interferences? *Bulletin of the Seismological Society of America*, 102 (6):2378–2391, 2012. doi: 10.1785/0120120066.

H E Bass, L N Bolen, Daniel Cress, Jerry Lundien, and Mark Flohr. Coupling of airborne sound into the earth: Frequency dependence. *The Journal of the Acoustical Society of America*, 67(5), 1980.

Markus Båth. *Spectral analysis in geophysics*. Amsterdam : Elsevier Scientific Pub. Co. ; New York : American Elsevier Pub, 1974. ISBN 0444412220 (American Elsevier).

John P Benoit and Stephen R McNutt. New constraints on source processes of volcanic tremor at Arenal Volcano, Costa Rica, using broadband seismic data. *Geophysical Research Letters*, 24(4):449–452, 1997.

Bernard Chouet. Dynamics of a Fluid-Driven Crack in Three Dimensions by the Finite Difference Method. *Journal of Geophysical Research*, 91(B14):13967–13992, 1986.

T Raju Damarla and David Ufford. Helicopter detection using harmonics and seismic-acoustic coupling. *SPIE Proceedings*, 6963, 2008. doi: 10.1117/12.776899.

Thyagaraju Damarla. Azimuth & Elevation Estimation using Acoustic Array. In *IEEE Xplore*, pages 1–7, 2010.

Silvio De Angelis and Stephen R McNutt. Observations of volcanic tremor during the January – February 2005 eruption of Mt. Veniaminof, Alaska. *Bulletin of Volcanology*, 69:927–940, 2007. doi: 10.1007/s00445-007-0119-4.

Robert P Dziak and Christopher G Fox. Evidence of harmonic tremor from a submarine volcano detected across the Pacific Ocean basin. *Journal of Geophysical Research*, 107 (B5):ESE 1–1—-ESE 1–11, 2002. doi: 10.1029/2001JB000177.

Eva P S Eibl, Christopher J Bean, Kristín Vogfjörd, and Aoife Braiden. Persistent shallow background microseismicity on Hekla volcano , Iceland : A potential monitoring tool. *Journal of Volcanology and Geothermal Research*, 289:224–237, 2014. ISSN 0377-0273. doi: 10.1016/j.jvolgeores.2014.11.004.

Páll Einarsson. Earthquakes and present-day tectonism in Iceland. *Tectonophysics*, 189 (1-4):261–279, April 1991. ISSN 00401951. doi: 10.1016/0040-1951(91)90501-I.

R. P. Feynman, R. B. Leighton, and M. L. Sands. *The Feynman lectures on physics.* Reading, Mass: Addison-Wesley Pub. Co., 1963.

Peter Franek, Jürgen Mienert, Stefan Buenz, and Louis Géli. Character of seismic motion at a location of a gas hydrate-bearing mud volcano on the SW Barents Sea margin. *Journal of Geophysical Research: Solid Earth*, pages 6159–6177, 2014. doi: 10.1002/2014JB010990.

K Grönvold, G Larsen, P Einarsson, S Þórarinsson, and K Sæ mundsson. The Hekla Eruption 1980-1981. *Bulletin of Volcanology*, 46-4:349–363, 1983.

Agust Gudmundsson, Niels Oskarsson, Karl Gronvold, Kristjan Saemundsson, Oddur Sigurdsson, Ragnar Stefansson, Sigurdur R Gislason, Pall Einarsson, Bryndis Brandsdottir, Gudrun Larsen, Haukur Johannesson, and Thorvaldur Thordarson. The 1991 eruption of Hekla, Iceland. *Bulletin of Volcanology*, 54(3):238–246, 1992.

M T Hagerty, S Y Schwartz, M A Garces, and M Protti. Analysis of seismic and acoustic observations at Arenal Volcano, Costa Rica, 1995 – 1997. *Journal of Volcanology and Geothermal Research*, 101:27–65, 2000.

Jay C. Hardin and Stanley L. Lamkin. Concepts for reduction of blade/ vortex interaction noise. *Journal of Aircraft*, 24(2):120–125, 1987. doi: 10.2514/3.45428.

Sandra I N Heleno, Bruno V E Faria, Zuleyka Bandomo, and João F B D Fonseca. Observations of high-frequency harmonic tremor in Fogo, Cape Verde Islands. *Journal of Volcanology and Geothermal Research*, 158:361–379, 2006. doi: 10.1016/j.jvolgeores.2006.06.018.

M Hellweg. Physical models for the source of Lascar's harmonic tremor. *Journal of Volcanology and Geothermal Research*, 101:183–198, 2000.

Ármann Höskuldsson, Níels Óskarsson, Rikke Pedersen, Karl Grönvold, Kristín Vogfjörð, and Rósa Ólafsdóttir. The millennium eruption of Hekla in February 2000. *Bulletin of Volcanology*, 70(2):169–182, April 2007. ISSN 0258-8900. doi: 10.1007/s00445-007-0128-3.

Alicia J Hotovec, Stephanie G Prejean, John E Vidale, and Joan Gomberg. Strongly gliding harmonic tremor during the 2009 eruption of Redoubt Volcano. *Journal of Volcanology and Geothermal Research*, 259:89–99, June 2013. ISSN 03770273. doi: 10.1016/j.jvolgeores.2012.01.001.

A Mark Jellinek and David Bercovici. Seismic tremors and magma wagging during explosive volcanism. *Nature*, 470(7335):522–5, February 2011. ISSN 1476-4687. doi: 10.1038/nature09828. URL `http://www.ncbi.nlm.nih.gov/pubmed/21350484`.

Philippe Jousset, Jürgen Neuberg, and Susan Sturton. Modelling the time-dependent frequency content of low-frequency volcanic earthquakes. *Journal of Volcanology and Geothermal Research*, 128:201–223, 2003. doi: 10.1016/S0377-0273(03)00255-5.

R Julian, U S Geological Survey, and Menlo Park. Volcanic tremor: Nonlinear excitation by fluid flow. *Journal of Geophysical Research*, 99(B6):11859–11877, 1994. doi: 10.1029/93JB03129.

Hiroyuki Kumagai, Pablo Palacios, Takuto Maeda, Diego Barba Castillo, and Masaru Nakano. Seismic tracking of lahars using tremor signals. *Journal of Volcanology and Geothermal Research*, 183(1-2):112–121, May 2009. ISSN 03770273. doi: 10.1016/j.jvolgeores.2009.03.010.

Kam W. Lo and Brian G. Ferguson. Broadband Passive Acoustic Technique for Target Motion Parameter Estimation. *IEEE Transactions on Aerospace and Electronic Systems*, 36(1):163–175, 2000.

Brendon Malovrh and Farhan Gandhi. Sensitivity of Helicopter Blade-Vortex-Interaction Noise and Vibration to Interaction Parameters. *Journal of Aircraft*, 42(3):685–697, 2005.

Stephen R. McNutt. Volcanic Tremor. *Encyclopedia of Earth Science*, 4:417–425, 1992.

Christian Müller, Vera Schlindwein, Alfons Eckstaller, and Heinrich Miller. Singing icebergs. *Science (New York, N.Y.)*, 310(5752):1299, November 2005. ISSN 1095-9203. doi: 10.1126/science.1117145.

Björn Olofsson. Marine ambient seismic noise in the frequency range 1–10 Hz. *The Leading Edge*, 29(4):418–435, 2010. doi: 10.1190/1.3378306.

B Pontoise and Y Hello. Monochromatic infra-sound waves recorded offshore Ecuador: possible evidence of methane release. *Terra Nova*, 14:425–435, 2002. doi: 10.1046/j.1365-3121.2002.00437.x.

T W Powell and J Neuberg. Time dependent features in tremor spectra. *Journal of Volcanology and Geothermal Research*, 128:177–185, 2003. doi: 10.1016/S0377-0273(03)00253-1.

Claudia Röösli, Fabian Walter, Stephan Husen, Lauren C. Andrews, Martin P. Lüthi, Ginny a. Catania, and Edi Kissling. Sustained seismic tremors and icequakes detected in the ablation zone of the Greenland ice sheet. *Journal of Glaciology*, 60(221):563–575, June 2014. ISSN 00221430. doi: 10.3189/2014JoG13J210.

A C Rust, N J Balmforth, and S Mandre. The feasibility of generating low-frequency volcano seismicity by flow through a deformable channel. *Geological Society, London, Special Publications 2008*, 307:45–56, 2008. doi: 10.1144/SP307.4.

Vera Schlindwein, Joachim Wassermann, and Frank Scherbaum. Spectral analysis of harmonic tremor signals at Mt. Semeru volcano, Indonesia. *Geophysical Research Letters*, 22(13):1685–1688, 1995.

Heidi Soosalu and Páll Einarsson. Earthquake activity related to the 1991 eruption of the Hekla volcano, Iceland. *Bulletin of Volcanology*, 63(8):536–544, January 2002. ISSN 0258-8900. doi: 10.1007/s00445-001-0177-y.

Heidi Soosalu, Páll Einarsson, and Bergþóra S. Þorbjarnardóttir. Seismic activity related to the 2000 eruption of the Hekla volcano, Iceland. *Bulletin of Volcanology*, 68(1):21–36, May 2005. ISSN 0258-8900. doi: 10.1007/s00445-005-0417-7.

Jacques Talandier and Emile A. Okal. Monochromatic T waves from underwater volcanoes in the pacific ocean: Ringing witnesses to geyser processes? *Bulletin of the Seismological Society of America*, 86(5):1529–1544, 1996.

Jacques Talandier, Olivier Hyvernaud, Emile a. Okal, and Pierre-Franck Piserchia. Long-range detection of hydroacoustic signals from large icebergs in the Ross Sea, Antarctica. *Earth and Planetary Science Letters*, 203(1):519–534, October 2002. ISSN 0012821X.

J. Paul Winberry, Sridhar Anandakrishnan, and Richard B. Alley. Seismic observations of transient subglacial water-flow beneath MacAyeal Ice Stream, West Antarctica. *Geophysical Research Letters*, 36(11):L11502, June 2009. ISSN 0094-8276. doi: 10.1029/2009GL037730.